MOLECULAR PHARMACOLOGY, 24:436–442

Structure-Activity Relationships of Cholinesterase Inhibitors

I. Quantum Mechanical Study of Affinities of Phenyl *N*-Methyl Carbamates

AMIRAM GOLDBLUM

Department of Pharmaceutical Chemistry, School of Pharmacy, Hebrew University of Jerusalem, Jerusalem 91120, Israel

Received March 14, 1983; Accepted June 14, 1983

SUMMARY

Ab initio self-consistent field-molecular orbitals-linear combination of atomic orbitals calculations of electrostatic potentials were performed in a few regions about some phenyl *N*-methyl carbamate derivatives. A similar active-site conformation was assumed and a low-energy common conformation was obtained from semiempirical perturbative configuration interaction over localized orbitals calculations. The results indicate that affinity constants of the carbamate derivatives used for this study may be an outcome of phenyl ring electrostatic interactions with the active site.

INTRODUCTION

The cholinesterase (EC 3.1.1.7) inhibitory activity of PNMCs[1] (Fig. 1) has been the subject of a few QSAR studies in recent years (1–5). Results were rationalized in terms of interaction mechanisms at the enzyme's active sites and subsites. A general outline of this reaction is (6):

$$ArOC + EH \overset{K_a}{\rightleftharpoons} [ArOC\text{--}EH] \overset{k_2}{\rightarrow} EC + ArOH \overset{k_3}{\rightarrow} EH + COH + ArOH \quad (1)$$

A substituted phenyl carbamate (*Ar*OC) reacts with the enzyme (*E*H) to form, first, a reversible complex with an affinity constant, K_a. Carbamylation of the enzyme (with rate constant k_2) leads to the inhibitory effect, since the regeneration of free enzyme (with rate constant k_3) is slow compared with the same step for the naturally acetylated enzyme. Most initial biological and biochemical work focused on values of pI_{50} and k_i (inhibition rate constant, $k_i = k_2K_a$), both of which are complex constants (7). Affinity constants, K_a (or their reciprocal constants, K_d), and carbamylation rate constants, k_2, have been resolved more recently (2–4, 6). Basing their argument on linear free energy correlation analysis, Nishioka *et al.* (3) proposed a binding mechanism involving hydrophobic, electronic, and steric factors. They found a biphasic dependence on electronic (Hammet's σ) effects and suggested a change in mechanism from rate-determining carbonyl protonation (electron-releasing substituents, $\rho < 0$) to nucleophilic attack on carbonyl (electron attractors, $\rho > 0$). Hetnarski and O'Brien (2) suggested that the aromatic moiety of PNMCs takes part in the binding mechanism as a π electron donor enhancing the formation of an active site charge-transfer complex. Ban and Nagata (8) calculated electronic indices of PNMCs at the π-electron Hückel theory level. They found a correlation between π density on ester and carbonyl oxygen with inhibitory (pI_{50}) potency and suggested that carbonyl-ester oxygen bond cleavage is rate-determining through hydrogen bonding of the ester oxygen to the active site.

It is clear that PNMCs are capable of participating in interactions in a few regions around them. The first step in any mechanism would be a close approach to the active site through noncovalent interaction forces. Although not necessarily rate-determining, interactions at this step may serve to identify subsequent ones. Such a "static" approach is most conveniently studied through MEP (9, 10). MEP has been a valuable tool for comparing protonation sites (11), localization of ions (12), and binding affinities (13) among molecules. In this paper we discuss the interactions of PMNC derivatives through their MEPs, these being derived from *ab initio* quantum mechanical calculations of their electronic structure in preferred, low-energy conformations.

METHODS

Three PNMC analogues were chosen for the study: the non-substituted analogue and its 2-methoxy and 2-cyano derivatives were found to have different affinities for housefly cholinesterase (4) (log $1/K_D$ = 3.92, 4.55, and 5.72, respectively) and to the bovine erythrocyte enzyme (3) (log $1/K_D$ = 2.70, 3.39, and 3.80, respectively). No difference was found among their k_2 values. The *ortho* substitutions are particularly attractive for calculation with regard to the combination of "steric" and

This research was supported in part by the Joint Research Fund of the Hebrew University and Hadassah.

[1] The abbreviations used are: PNMC, phenyl *N*-methyl carbamate; QSAR, quantitative structure-activity relationships; MEP, molecular electrostatic potential; PCILO, perturbative configuration interaction over localized orbitals; STO, Slater-type orbitals; HOMO, highest occupied molecular orbital; LEMO, lowest empty molecular orbital.

0026-895X/83/060436-07$02.00/0

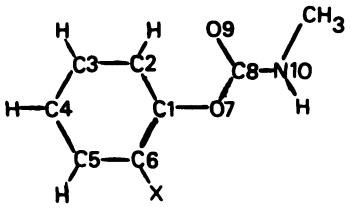

1A. X=H

1B. X=CN

1C. X=OCH_3

FIG. 1. *PNMCs used for the study*

"electronic" effects they may have on the carbamate group, limiting its conformational freedom in comparison to the effect of *meta* and *para* substituents.

From the point of view of "classical QSAR" they represent a wide range of "Hammet type" electronic effect (14) (σ^0 = 0.0, −0.16, and 0.69; σ_p = 0.0, −0.27, and 0.66, respectively) and a small range of hydrophobic character, as represented by Hansch's π values (3, 15).

Energy dependence on carbamate group conformation was studied by PCILO (16). Input geometries were taken from an X-ray study of 4-methylthio-3,5-dimethyl PNMC (17) by changing the appropriate groups with hydrogen atoms at standard bond lengths (18) whereas other substituents' bond lengths and angles were optimized by PCILO.

Assuming "rigid" receptor requirements for interaction with substrates, we chose a single, common PNMC conformation to compare the molecules under a similar active-site orientation. The minimal ("best") conformation found by PCILO for *1A* was chosen, since it was closer to the experimental X-ray conformation of an effective PNMC inhibitor (17), and this conformation was also a low one for *1B* and *1C*, although somewhat higher in energy than their own minima (by approximately 4 and 1 Kcal, respectively). Interaction energies at the active site may easily compensate for this change in conformation required of *1B* and *1C*. The similar conformations used for electrostatic potential comparisons are *1A*, *1B1*, and *1C1*, but *ab initio* wave functions were calculated also for *1B* and *1C* in their own minimal PCILO conformations for comparative reasons. STO-3G minimal basis set was used for all *ab initio* calculations, by Gaussian 76′ (19).

The electrostatic potential at a point P in space could then be calculated by integrating the electron density function $\rho(j)$ derived from the *ab initio* molecular orbitals (of *1A*, *1B1*, and *1C1*) and the nuclear charges Z_i:

$$V(P) = \sum_{i=1}^{n} \frac{Z_i}{r_{ip}} - \int \frac{\rho(j)\, d\tau_j}{r_{jp}} \qquad (2)$$

the i index being over nuclei and the j over electrons (9). The MEP

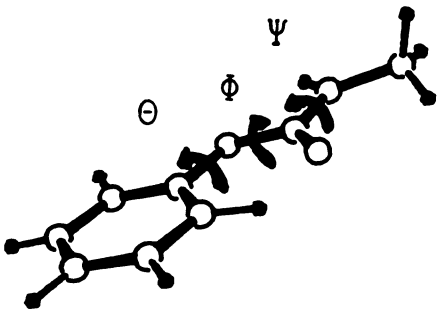

FIG. 2. *Definition of dihedral angles for the carbamates*

Here $\theta = \phi = 0°$ and $\psi = 180°$. Angles increase in a counterclockwise direction when viewed from the phenyl ring outward along the relevant bonds.

was calculated in three planes, which may be important for noncovalent interactions: the amide group plane, a plane parallel to the aromatic ring, and the one parallel to the amide group. Parallel planes were calculated at a distance of 2 Å, longer than required for covalent bond formation, so that the electrostatic component will determine the ranking of the total energy of interaction with the different molecules. Difference maps were produced for clearer evaluation of the relative changes for different molecules. We also studied the electrostatic potential of the two "lone pair" carrying substituents, along their assumed directions in space.

All calculations were carried on a CDC Cyber 74′ at the Hebrew University computation center in Givat Ram, Jerusalem.

RESULTS AND DISCUSSION

Conformations of the carbamate groups. The starting geometry for PNMC and the definition of dihedral angles are shown in Fig. 2. Values for θ-ϕ, θ-ψ (ϕ = 0°), and $\psi(\theta_{min}, \phi_{min})$ energy dependence were calculated in intervals of 20°. Figure 3 shows the θ-ϕ energy map for the nonsubstituted compound (*1A*), and Fig. 4 is its 3-dimensional representation. It is readily seen from Figs. 3 and 4 that the "free" molecule is expected to have conformational freedom in the range of the "energy valley" θ = 210°–270° and ϕ = 0° ± 20°.

The lack of "symmetry" for $\theta = 180° \pm \Delta\theta$ results from localization of aromatic double bonds in PCILO. Figure 5 presents the energy dependence of θ-ψ variations, and Fig. 6 is its 3-dimensional equivalent. The ψ dependence is nearly constant for different θ values, with a $\Delta H^{\neq}$ value of 12–13 Kcal as rotation barrier for the carbonyl-nitrogen bond. An experimental value, $\Delta H^{\neq}$ = 15.5 Kcal, was found for this barrier in *N,N*-dimethylphenyl carbamate (in CCl_4, 25°) (20). The ψ energy increase is a result of the decrease in "delocalization energy" obtained by the

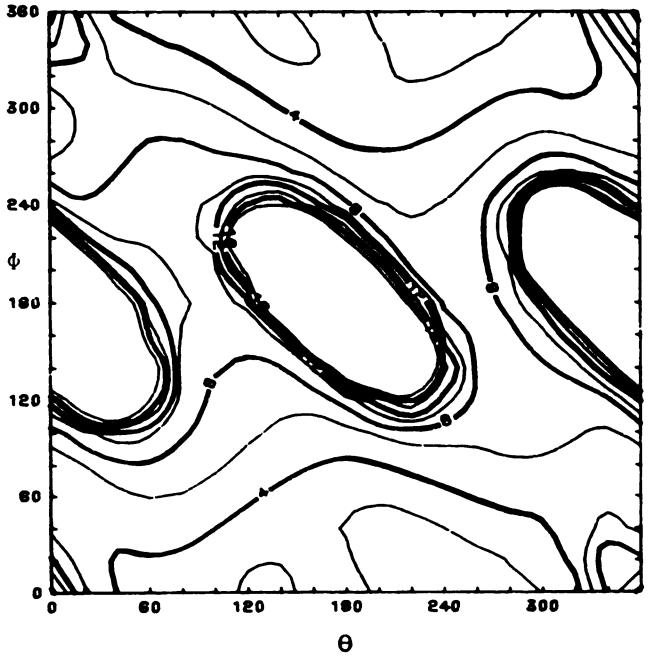

FIG. 3. *Conformational energy map of 1A: 20° variations of θ and ϕ*

Values are in kilocalories above the minimum. Energies of 20 Kcal or more above the minimum were equated to 20 Kcal; 2 Kcal separate nearest lines.

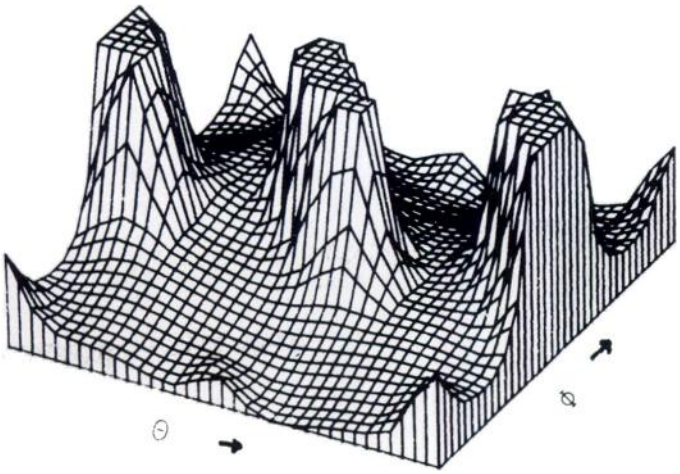

FIG. 4. *Three-dimensional representation of θ-φ energy variations in 1A*
Additional lines every 10° were interpolated.

PCILO energy decomposition scheme. The minimal energy conformation of *1A* is shown in Fig. 7.

The localized character of PCILO calculations requires user definition of double bonds, so that two Kekulé structures were used for the calculation of conformational energy maps of the 2-CN (*1B*) and 2-OMe (*1C*) derivatives. Both Kekulé pairs showed similar θ-ϕ energy dependence with minor differences. Figure 8 presents the θ-ϕ map for *1B*. The 2-CN derivative clearly has a more restricted conformational freedom than does *1A* in Fig. 3. Minimal regions are found along "canyons" near the map's corners, the lowest one being $\theta = \phi = 20°$ (Fig. 9). A θ-ϕ map (Fig. 10) for *1C* shows behavior closer to that of *1A*, with restricted regions about $\theta = \phi = 0° \pm 40°$. The minimal energy conformer is drawn in Fig. 11. The θ-ψ dependence for *1B* and *1C* was found to be similar to that of *1A*.

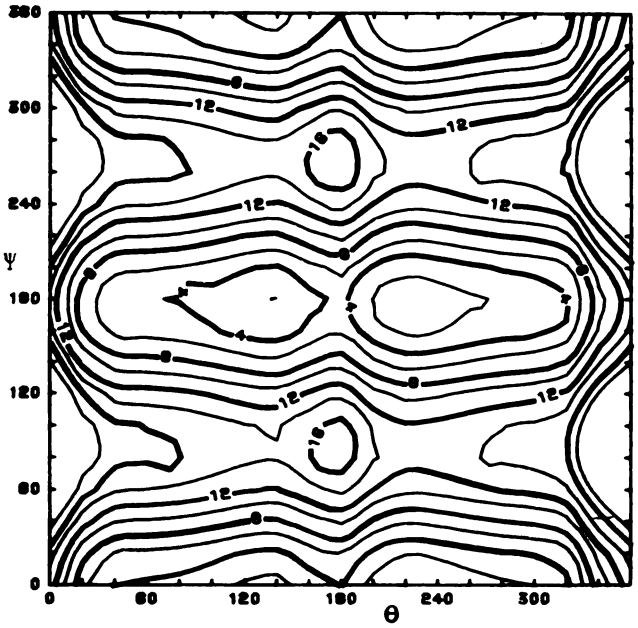

FIG. 5. *Conformational map for θ-ψ energy variations of 1A*

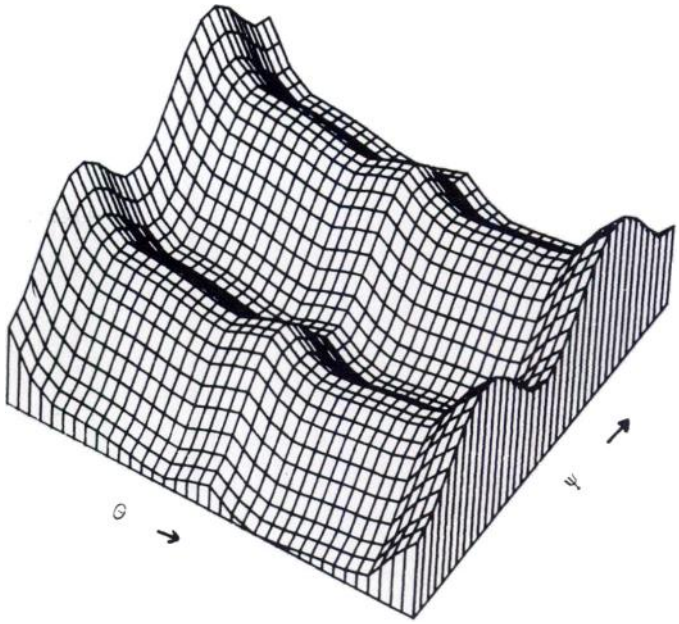

FIG. 6. *Three-dimensional map of θ-ψ energy variations of 1A*

The X-ray structures published for some PNMC derivatives correspond closely to the minimal conformations of *1A* and *1C*. Mesurol (17) has the carbonyl carbon atom at approximately 60° with respect to the aromatic plane ($\theta = 0° \pm 60°, 180° \pm 60°$), and the carbonyl oxygen atom is in the plane of the ring—O—C bonds ($\phi \cong 0°$). The solid-phase conformation was not found to be influenced by short intermolecular distances to nearby molecules (16), thus being of greater value for comparison with the "free molecule" calculation. Closely related values were found for physostigmine (21) ($\theta = 77°$, $\phi = 5°$), whereas neostigmine bromide (22) ($\phi = 26°$, $\phi = 5°$) was closer to *1B*.

Exner and Bláha (23) found *N*-methyl carbamate conformation (dipole moment in benzene) to be mainly *Z,Z* (Fig. 12), without excluding the presence of *E* within the amide grouping. PCILO calculations (Figs. 5 and 6) indicate a small energy difference between *Z* and *E* of the amide group ψ dependence. The calculations also show (Fig. 7) that the minimal "gas phase" conformation of the parent PNMC is nonplanar, deviating from a planar *Z,Z* conformation. Results of "gas phase" calculations may be compared roughly with experimental results in nonpolar solvents such as benzene and CCl_4.

Electronic (ab initio) structure of PNMC derivatives. STO-3G wave functions were calculated for *1A*, *1B*, and *1C* in their own PCILO minimal energy conformations and for *1B* and *1C* in the minimal (assumed receptor)

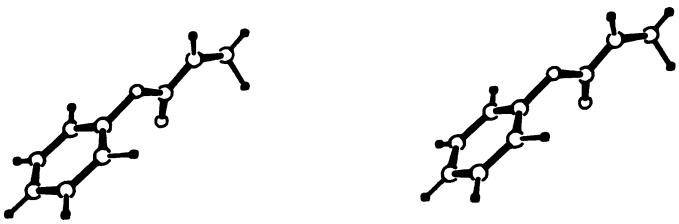

FIG. 7. *Stereo drawing of the minimal energy conformation of 1A*

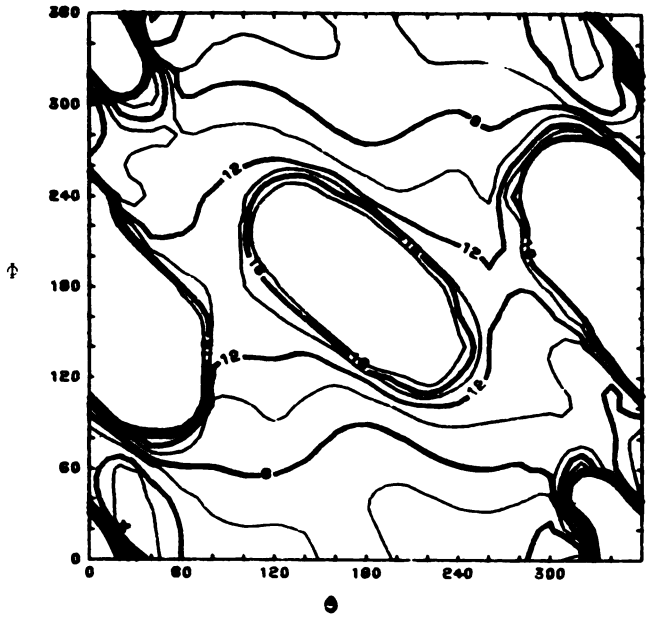

FIG. 8. *θ-φ energy variations of 1B*
The minimum (20°, 20°) is indicated by +.

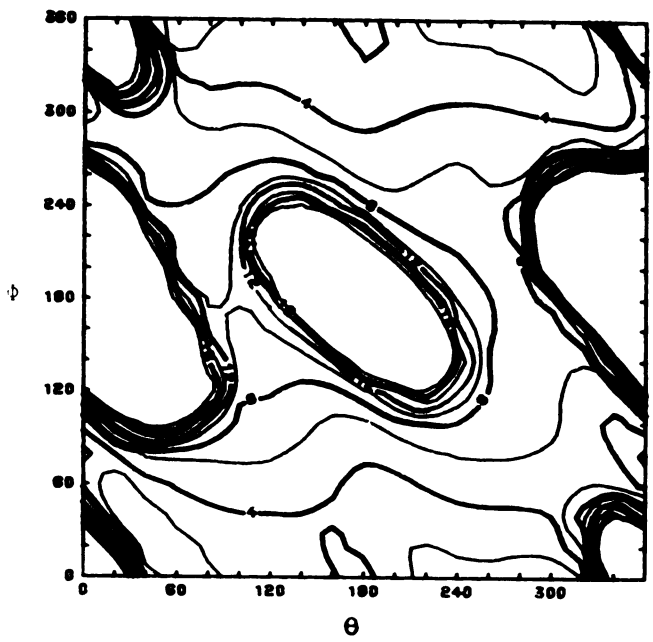

FIG. 10. *θ-φ energy variations of 1C*

conformation of *1A* (*1B1* and *1C1*). HOMO are π-aromatic of symmetry E_1 but include participation of the ester oxygen atom near the ring. The nitrile and methoxy substituents also participate significantly in HOMO orbitals. HOMO-1 is also π for *A* and *C*, and the carbamate group orbitals are HOMO-1 for *B* and HOMO-2 in *A* and *C*. LEMO and LEMO + 1 are pure π aromatic of symmetry E_2 with no participation of carbamate orbitals. LEMO + 2 are nearly pure carbamate orbitals in all molecules. Mulliken charge distribution (Table 1) reflects the small variations among similar atoms in the various molecules and seems inadequate to resolve the differential affinity. The largest variations were found on C-6 (Fig. 1). The charge distribution on the carbamate group was nearly constant (standard deviation ±0.003), the only exception being a lower carbonyl oxygen density for *1B*.

MEPs. MEPs were calculated for the "receptor conformation" of the three molecules (conformations *1A*, *1B1*, and *1C1*) based on their STO-3G wave functions. Three regions around each molecule were explored at grid points, and maps were drawn by interpolation. All difference maps were produced by subtracting the values, at grid points, of the substituted from the nonsubstituted analogous regions.

Atomic positions in the maps (Figs. 13–18) are designated by small plus signs. Figure 13 shows the MEP of *1A* in the plane of the carbamate group, and Fig. 14 presents the difference maps for the 2-cyano (*1B1*) and 2-methoxy (1C1) derivatives, both in a similar conformation as *1A*, of the carbamate group. The carbonyl atoms are in the center of the maps, pointing toward the *tops* of the figures. The *N*-methyl group is to the *right* of the carbonyl.

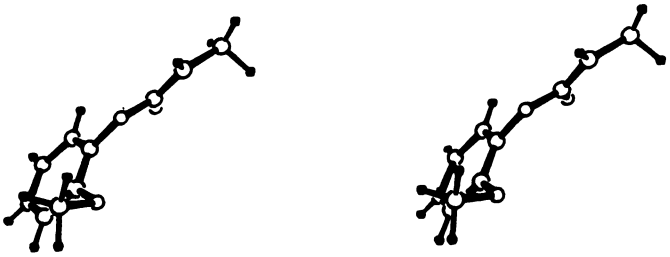

FIG. 11. *Stereo drawing of the minimal energy conformer of 1C*

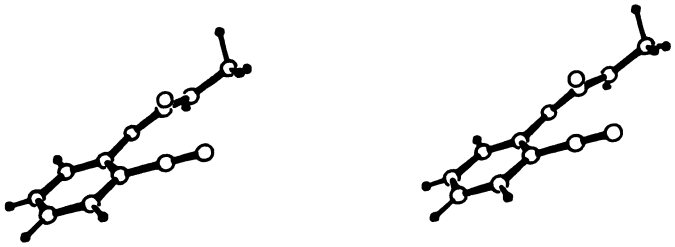

FIG. 9. *Stereo drawing of the minimal energy conformer of 1B*

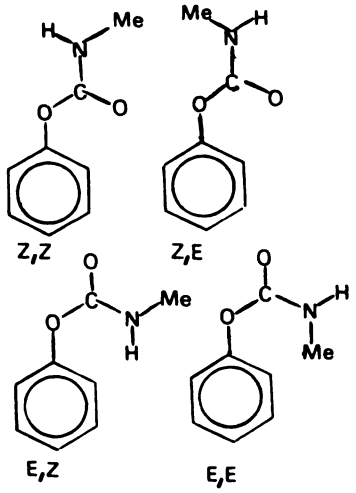

FIG. 12. *Planar conformational possibilities of PNMC derivatives*

TABLE 1

Mulliken ab initio net charges on atoms

Atom[a]	Molecule				
	1A	*1B*	*1B1*	*1C*	*1C1*
C-1	0.139	0.159	0.156	0.118	0.121
C-2	−0.092	−0.096	−0.088	−0.087	−0.085
C-3	−0.067	−0.052	−0.055	−0.077	−0.076
C-4	−0.077	−0.080	−0.074	−0.074	−0.071
C-5	−0.062	−0.040	−0.045	−0.090	−0.090
C-6	−0.083	−0.022	−0.008	0.122	0.124
O-7	−0.280	−0.276	−0.273	−0.271	−0.275
C-8	0.447	0.455	0.451	0.449	0.450
O-9	−0.322	−0.299	−0.319	−0.323	−0.323
N-10	−0.386	−0.380	−0.383	−0.385	−0.385
C-11[b]	−0.186	−0.184	−0.185	−0.185	−0.186
X[c]	—	0.065	0.074	−0.248	−0.248
Y[d]	—	−0.187	−0.189	−0.051	−0.051
$H^{e}_{N\text{-}10}$	0.235	0.233	0.239	0.237	0.235
Dipole moment Debyes (calc.)	1.706 Exp. 2.81[f]	3.922	2.769	2.193	2.331

[a] Numbers of atoms refer to those in Fig. 1.
[b] *N*-Methyl carbon atom.
[c] Cyano carbon atom of *1B* and *1B1*, methoxy oxygen atom of *1C* and *1C1*.
[d] Cyano nitrogen atom of *1B* and *1B1*, methoxy carbon atom of *1C* and *1C1*.
[e] Amide hydrogen atom.
[f] Ref. 23.

The largest interaction of *1A* with a positive point charge (q = +1) is about −62 Kcal. *1B1* has a less negative potential in this region (by 4–6 Kcal.) and *1C1* is more negative (by 1–2 Kcal). We interpret these results as indicating that protonation of carbonyl oxygen or hydrogen binding to it do not sort the order of affinities ($B > C > A$) and thus do not operate at this step or have only minor influence. We also draw attention to the inadequacy of the localized charge distribution (Table 1) to follow even qualitatively the theoretical results with the "full" molecular electrostatic potential. We do not attach much importance to the exact potential values, based on the assumption of a full positive charge inter-

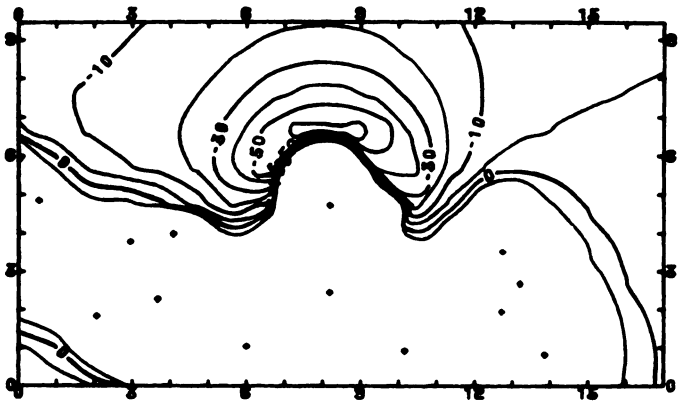

FIG. 13. *MEP of 1A in the plane of the carbamate group*
Atomic positions, to scale, are indicated by +. Axes are numbered in Bohr radius units.

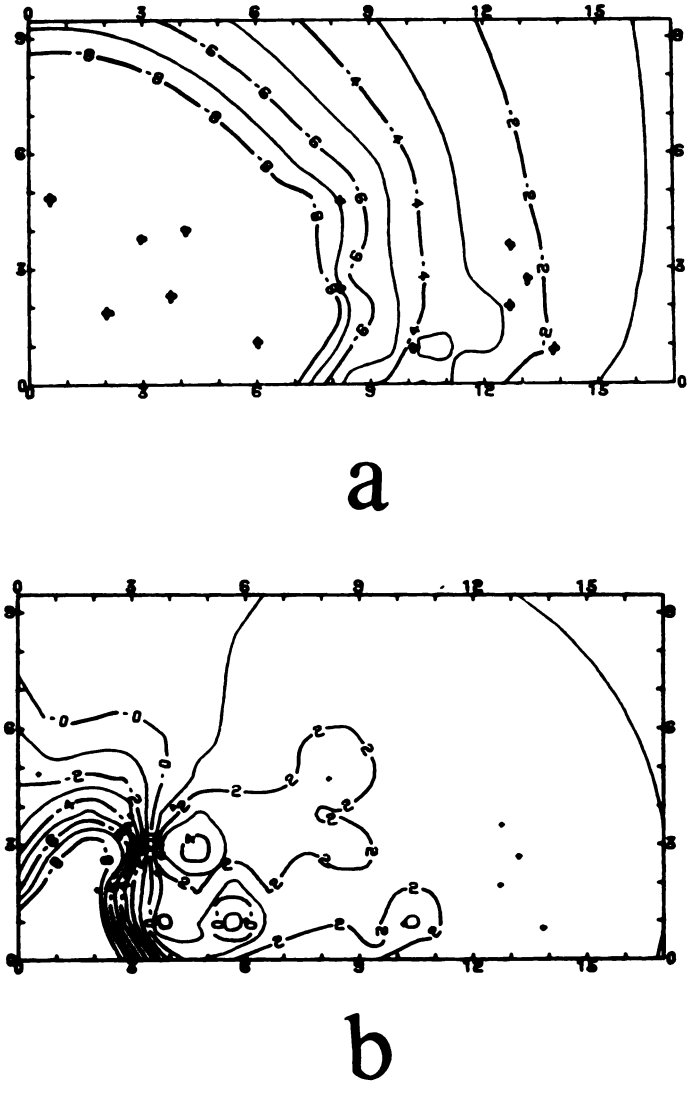

FIG. 14. *Difference MEP maps in the plane of the carbamate group* a, *1B1*; b, *1C1*.

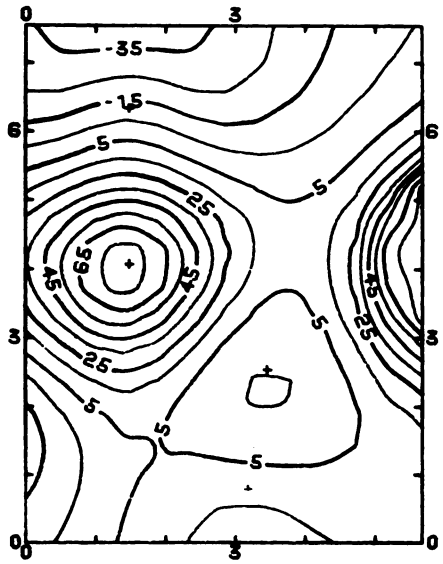

FIG. 15. *MEP of 1A in a plane parallel to the amide group at a distance of 2 Å*

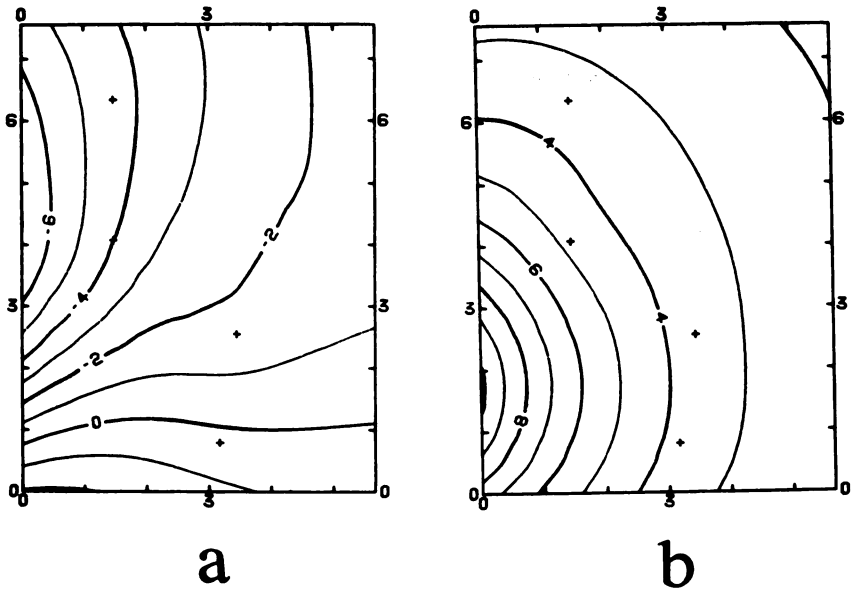

FIG. 16. *Difference MEP maps in a plane parallel to t'.e amide group at a distance of 2 Å*
a, *1B1*; b, *1C1*.

acting with the molecules. The ranking is still expected to be valid.

Figure 15 presents the electrostatic potential of *1A* in a plane parallel to the amide group at a distance of 2 Å from it. From this region in the active site we expect a charged nucleophile to attack the carbonyl. The uncertainty in predicting nucleophilic attack by MEP was recently explained (24). Some of this uncertainty is relieved when the nucleophile is negatively charged and the interaction calculated at distances larger than ground-state covalent bond lengths.

The high repulsive potential of ~80 Kcal (above the carbon of the carbonyl, with oxygen toward the *top* of the figure) is reversed in sign for interaction with a nucleophile carrying a full or partial negative charge (for which the absolute value may be much smaller). Figure 16 shows the difference maps for the cyano (*1B1*) and methoxy (*1C1*) derivatives. As expected by "intuitive classical chemistry," the potential for negatively charged nucleophilic interaction with the carbonyl of *1B1* is stronger (by ~4 Kcal at this distance, for a fully negative point change) and weaker for a similar attack on *1C1* (by ~5 Kcal).

There is overwhelming evidence for the existence of nucleophilic attack on the carbonyl at some stage of the inhibition process, but, unless there is a change in the electronic structure of the reactants prior to binding, we doubt the importance of such an interaction to the affinity.

Maps for the plane parallel to the phenyl ring are shown in Figs. 17 (for *1A*) and 18 (difference maps for *1B1* and *1C1*). Interaction with a fully developed negative charge is stronger (by 8–10 Kcal) above the ring of the 2-cyano (*1B1*) derivative and also for the 2-methoxy derivative (by ~2–10 Kcal). It is repulsive for the "parent" (*1A*) compound. This type of interaction follows the experimental order ($B > C > A$). The energies of interaction will naturally depend upon the distance and charges of the active site group interacting with the ring. Energy differences should be smaller to correspond to variations in affinities.

Iwata and Morokuma (25) suggested that the electrostatic energy is often a good indicator of the hydrogen bond energy, in a qualitative sense and with a scaling factor which is less than unity. Keeping those restrictions in mind, we calculated the potential along the "extension" of lone pairs in *1B1* and *1C1*.

The possibility of hydrogen bonding by the cyano and methoxy substituents strengthens the above tendencies in the direction of the experimental results. This ability was calculated along the continuation line of the C≡N bond (of *1B1*), and a minimum (−72.9 Kcal at 1.1 Å from nitrogen) was found. We assumed an angle of 110° (ring carbon—O—lone pair) and dihedral angles (of methoxy methyl group ± 120°) for the methoxy group lone pairs.

The minimal value for the lone pair in the aromatic ring plane, (in the same general direction as the cyano

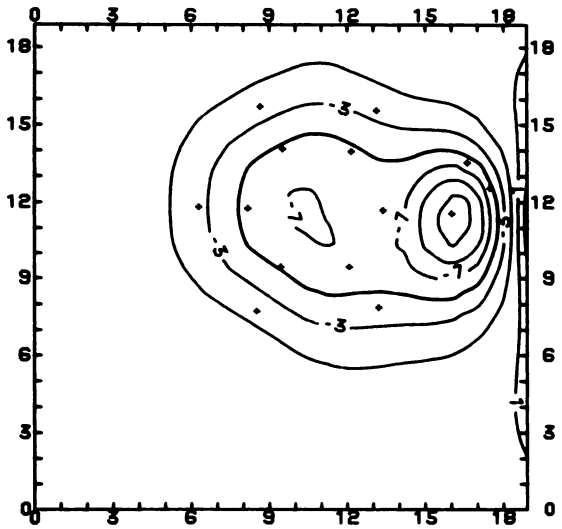

FIG. 17. *MEP of 1A in a plane parallel to the phenyl ring at a distance of 2 Å*

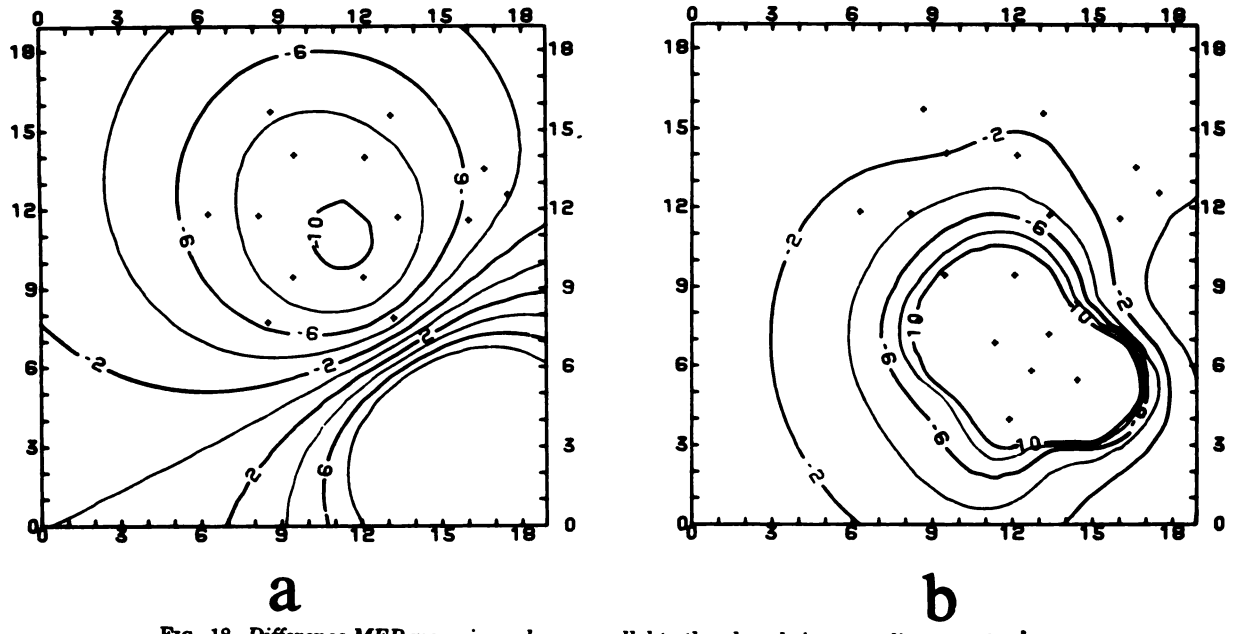

FIG. 18. *Difference MEP maps in a plane parallel to the phenyl ring at a distance of 2 Å* a, *1B1*; b, *1C1*.

group minimum) was −56 Kcal at 1 A from oxygen. Again, one should remember that those values describe the interaction with a fully developed positive charge, which is probably not the case inside the active site.

We conclude by suggesting that the affinities of carbamates for the active site of bovine and housefly cholinesterases are mainly the outcome of electrostatic interaction with the phenyl ring at a limited common conformation for the various PNMC derivatives. This interaction may be enhanced (or in some cases determined) by hydrogen bonding of the active site to the substituents. At this stage, we cannot discuss the contribution of steric and lipophilic interactions, which must have their own influence on the affinities.

ACKNOWLEDGMENTS

We appreciate the time and effort spent by staff of the Hebrew University Computation Center—Zvi Kidron, Yuppi Herzman, Simon Shickman, and Shlomit Felix, who helped to implement, test, and run the various programs used for this study and who never failed to give good advice.

REFERENCES

1. Hansch, C., and E. W. Deutsch. The use of substituent constants in the study of structure-activity relationships in cholinesterase inhibitors. *Biochim. Biophys. Acta* **126**:117–128 (1966).
2. Hetnarsky, B., and R. D. O'Brien. Electron donor and affinity constants and their application to the inhibition of acetylcholinesterase by carbamates. *J. Agric. Food Chem.* **23**:709–713 (1975).
3. Nishioka, T., T. Fujita, K. Kamoshita, and M. Nakajima. Mechanism of inhibition reaction of acetylcholinesterase by phenyl *N*-methyl carbamates. *Pestic. Biochem. Physiol.* **7**:107–121 (1977).
4. Kamoshita, K., I. Ohno, T. Fujita, T. Nishioka, and M. Nakajima. Quantitative structure-activity relationships of phenyl *N*-methyl carbamates against housefly and its acetylcholinesterase. *Pestic. Biochem. Physiol.* **11**:83–103 (1979).
5. Goldblum, A., M. Yoshimoto, and C. Hansch. Quantitative structure-activity relationships of phenyl *N*-methyl carbamate inhibition of acetylcholinesterase. *J. Agric. Food Chem.* **29**:277–288 (1981).
6. Hastings, F. L., A. R. Main, and F. Iverson. Carbamylation and affinity constants of some carbamate inhibitors of acetylcholinesterase and their relation to analogous substrate constants. *J. Agric. Food Chem.* **18**:497–502 (1970).
7. O'Brien, R. D. Acetylcholinesterase and its inhibition, in *Insecticide Biochemistry and Physiology* (C. F. Wilkinson, ed.). Plenum Press, New York, 271–296 (1976).
8. Ban, T., and C. Nagata. The electronic structure of carbamate derivatives as the inhibitors of cholinesterase. *Jpn. J. Pharmacol.* **15**:32–38 (1965).
9. Bonaccorsi, R., E. Scrocco, and J. Tomasi. Molecular self-consistent-field calculations for ground state of some 3-membered ring molecules. *J. Chem. Phys.* **52**:5270–5284 (1970).
10. Scrocco, E., and J. Tomasi. Electronic molecular structure, reactivity and intermolecular forces: an euristic interpretation by means of electrostatic molecular potentials. *Adv. Quantum Chem.* **2**:115–193 (1978).
11. Bonaccorsi, R., A. Pullman, E. Scrocco, and J. Tomasi. The molecular electrostatic potential for the nucleic acid bases: adenine, thymine and cytosine. *Theor. Chim. Acta* **24**:51–60 (1972).
12. Pullman, B., A. Goldblum, and H. Berthod. Anion binding to nucleic acid bases: a quantum mechanical exploration using electrostatic molecular potentials. *Biochem. Biophys. Res. Commun.* **77**:1166–1169 (1977).
13. Agresti, A., F. Buffoni, J. J. Kaufman, nd C. Petrongolo. Structure-activity relationships of eseroline and morphine: *ab initio* quantum-chemical study of the electrostatic potentials and of the interaction energy with water. *Mol. Pharmacol.* **18**:461–467 (1980).
14. Hansch, C., and A. Leo. *Substituent Constants for Correlation Analysis in Chemistry and Biology*. Wiley Interscience, New York (1979).
15. Fujita, T., K. Kamoshita, T. Nishioka, and M. Nakajima. Physicochemical parameters for structure-activity studies of substituted phenyl *N*-methyl carbamates. *J. Agric. Biol. Chem.* **38**:1521–1528 (1974).
16. Diner, S., J. P. Malrieu, F. Jordan, and M. Gilbert. Localized bond orbitals and the correlation problem. III. Energy up to the third order in the zero differential overlap approximation. *Theor. Chim. Acta* **15**:100–124 (1969).
17. Takusagawa, F., and R. A. Jacobson. Crystal and molecular structure of carbamate insecticides. I. Mesurol. *J. Agric. Food Chem.* **25**:329–333 (1977).
18. *Tables of Interatomic Distances and Configuration in Molecules and Ions*. The Chemical Society, London, Special Publication 18 (1965).
19. Hehre, W. J., R. F. Stewart, and J. A. Pople. Self consistent molecular orbital methods. I. Use of Gaussian expansions of slater-type atomic orbitals. *J. Chem. Phys.* **51**:2657–2664 (1969).
20. Macháček, V., and M. Večeřa. Study of hindered rotation about C-N bonds in carbamates. *Collect. Czech. Chem. Commun.* **37**:2928–2932 (1972).
21. Pauling, P., and T. J. Pletcher. Crystal and molecular structure of eserine. *J. Chem. Soc. Perk. Trans.* **II**:1342–1345 (1973).
22. Pauling, P., and T. J. Pletcher. Inhibitors of acetylcholinesterase: crystal structure of neostigmine bromide. *J. Med. Chem.* **14**:1–2 (1971).
23. Exner, O., and K. Bláha. The conformation of aromatic carbamates in solution: a dipole moment study. *Collect. Czech. Chem. Commun.* **42**:2379–2387 (1977).
24. Politzer, P., and K. C. Daiker. Models for chemical reactivity, in *The Force Concept in Chemistry* (B. M. Deb, ed.). Van Nostrand-Reinhold Inc., New York, 294–387 (1981).
25. Iwata, S., and K. Morokuma. Molecular orbital studies of hydrogen bonds, part V. *J. Am. Chem. Soc.* **95**:7563–7575 (1973).

Send reprint requests to: Dr. Amiram Goldblum, Department of Pharmaceutical Chemistry, School of Pharmacy, Hebrew University of Jerusalem, P.O. Box 12069, Jerusalem 91120, Israel.